

BEAM STACK SEARCH-BASED RECONSTRUCTION OF UNHEALTHY CORONARY ARTERY WALL SEGMENTATIONS IN CCTA-CPR SCANS

Antonio Tejero-de-Pablos^{*†} Hiroaki Yamane^{†*} Yusuke Kurose^{*†}
 Junichi Iho[†] Youji Tokunaga[†] Makoto Horie[†] Keisuke Nishizawa[†]
 Yusaku Hayashi[†] Yasushi Koyama^{††} Tatsuya Harada^{*†}

^{*} The University of Tokyo RCAST, Meguro 153-0041, Tokyo, Japan

[†] RIKEN Center for Advanced Intelligence Project, Chuo 103-0027, Tokyo, Japan

[‡] Sakurabashi Watanabe Hospital, Kita 530-0001, Osaka, Japan

ABSTRACT

The estimation of the coronary artery wall boundaries in CCTA scans is a costly but essential task in the diagnosis of cardiac diseases. To automatize this task, deep learning-based image segmentation methods are commonly used. However, in the case of coronary artery wall, even state-of-the-art segmentation methods fail to produce an accurate boundary in the presence of plaques and bifurcations. Post-processing reconstruction methods have been proposed to further refine segmentation results, but when applying general-purpose reconstruction to artery wall segmentations, they fail to reproduce the wide variety of boundary shapes. In this paper, we propose a novel method for reconstructing coronary artery wall segmentations, the Tube Beam Stack Search (TBSS). By leveraging the voxel shape of adjacent slices in a CPR volume, our TBSS is capable of finding the most plausible path of the artery wall. Similarly to the original Beam Stack Search, TBSS navigates along the voxel probabilities output by the segmentation method, reconstructing the inner and outer artery walls. Finally, skeletonization is applied on the TBSS reconstructions to eliminate noise and produce more refined segmentations. Also, since our method does not require learning a model, the lack of annotated data is not a limitation. We evaluated our method on a dataset of coronary CT angiography with curved planar reconstruction (CCTA-CPR) of 92 arteries. Experimental results show that our method outperforms the state-of-the-art work in reconstruction.

Index Terms— Artery wall reconstruction, Beam Stack Search, CPR coronary CT angiography, noisy segmentations

1. INTRODUCTION

The automation of the diagnosis of coronary artery diseases is essential in order to fight what is one of the main causes of death worldwide. Such diagnosis begins in many cases with the extraction of the coronary arteries from a Coronary Computed Tomography Angiography (CCTA) to look for anomalies

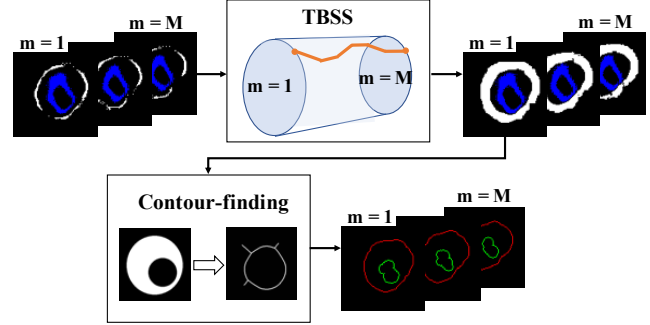


Fig. 1. Our TBSS traverses the segmentations of an artery wall boundary (inner in blue/green and outer in white/red) section of M slices, looking for the most probable voxel paths between consecutive slices.

lies. Anomalies such as plaques and stenosis [1] are best observed in Curved Planar Reformation (CPR) volumes, which map the artery walls following a straight line as in a “pipe” or a “tube”. Then, the boundaries of the artery wall are estimated, but this is an arduous and error-prone task for which many efforts to automate it have been done.

In [2], a graph convolutional neural network is used to predict a mesh for segmentation of the lumen (inner boundary wall). Similarly, in [3] a convolutional recurrent neural network is used to segment the artery wall, but neither of the aforementioned, nor the majority of artery segmentation works, deal with both the inner and outer boundaries of the wall. The simultaneous segmentation of inner and outer boundaries was tackled in [4] by combining region growing with level sets, and in [5] by using a hybrid UNet-based convolutional neural network (CNN). The outer boundary of the vessel is harder to segment due to its blurriness and its highly-variable geometry, as it may include plaques and bifurcations [6]. Indeed, the aforementioned methods suffer from early termination of the artery and “holes” in the segmented wall.

Not limited to the coronary arteries, since automatic segmentations of body organs are affected by noise and image artifacts, a number of reconstruction methods have been proposed. On the one hand, some methods attempt incorporating refining during the training process of a segmentation CNN. In [7], a segmentation UNet is used along a conditional variational autoencoder to learn a latent space of plausible segmentations given an ambiguous image. However, it requires multiple annotations per image in order to be trained, which is costly. In [8], shape priors of the segmented organ are learned in order to restrict the shape of the segmentations (e.g., “a heart is oval-shaped”). These methods cannot be applied once the training is finished, that is, when the segmentation results have been already obtained. To solve this, on the other hand, post-processing methods that are independent of the segmentation method and annotations were proposed [9][10][11]. They try to minimize a function that models the noise-free version of the input segmentation, and were successfully applied to medical image. Among them, the state-of-the-art performance is provided by Post-DAE [11], which employs a denoising autoencoder to reconstruct anatomically plausible segmentations from erroneous ones.

However, reconstructing segmentations of a CCTA-CPR coronary artery wall boundary is especially complex. The aforementioned problems (i.e., blurry Hounsfield Unit values and high-variance in the shape produced by anomalies in the artery) cause artifacts in segmentation results that are hard to refine using previous post-processing methods. In this paper, we present the tube beam stack search (TBSS), a post-processing method capable of reconstructing erroneous results output by a coronary artery wall segmentation method. Figure 1 shows an example of an uncertain section of the segmented artery wall, where boundary voxels disappear gradually to reappear later. By leveraging the shape of adjacent cross-sections, our TBSS is capable of finding the most plausible path of the artery wall, filling missing voxels and reshaping the boundary. As this method does not require learning a model, it does not suffer from neither the lack of data nor the imbalanced class problems (in boundary segmentation, the background class represents the vast majority of voxels).

2. TUBE BEAM STACK SEARCH (TBSS)

TBSS leverages the continuity among adjacent images to perform image completion; that is, even if the segmented boundary contains a “hole” in the wall, there must be a continuity in the tube wall. Also, while other methods rely on the “known” shape of the segmented organ in a single image, TBSS does not assume any shape prior. This allows adjusting to the variable shapes of unhealthy artery wall sections, which, unlike the healthy ones, are often irregular. Our method is based on the beam stack search algorithm [12]. This algorithm explores a graph by expanding the most promising node in a limited set, integrating systematic backtracking to find an op-

timal solution. It became popular after its application in machine translation, and its capability to find the most probable “path” along a set of candidates makes it suitable for our case. The extrapolation of this concept to the medical image reconstruction problem is not trivial; this section explains the ingenuity behind our implementation.

TBSS attempts to find voxel *paths* with the highest probability in a segmented artery section. We hypothesize we can determine the existence of artery wall boundary voxels even if the segmentation is uncertain. We refer to the output of the segmentation network (i.e., our input) as *probability maps*. Each probability map contains the probability of each voxel of a cross-section (or *slice*) of an artery of being a boundary. Since searching in the whole artery length is unfeasible, due to the exponential growth of possible paths, we divide the search problem in smaller artery sections, as probability maps away from each other are unlikely to be related. Also, our setting considers that the artery wall consists of two boundaries, the inner (lumen) and outer (outside) boundaries.

The performance of TBSS can be controlled with a set of hyperparameters:

- Length M : Length of the segmented artery section.
- Threshold T : Minimum acceptable value for the cumulative probability along the search *path*. The threshold for the inner and outer boundaries can be different.
- Beam B : Size of the voxel neighborhood for a path in P_m ($m \neq 1$).
- Stack S : For a certain path in P_m ($m \neq 1$), maximum number of candidate voxels to explore inside the neighborhood ($S \geq B$).

TBSS is applied separately for the inner and outer boundaries on both directions; not only from the probability map 1 to M , but also from M to 1. Then, the reconstructions in both directions are merged slice by slice, by following a priority rule for voxels with a different value: *inner boundary* > *outer boundary* > *background*. This has two effects: it finds paths that cannot be found in only one direction, and it alleviates the fading of the reconstruction (only a subset of the paths reaches the last slice). An ablation study on the sensitivity of each hyperparameter and the reverse reconstruction on the reconstruction results is provided on our website¹.

The flow of our TBSS algorithm is as follows (the pseudo-code is provided on our website¹). Let $I = \{I_1 \dots I_N\}$ be the input segmentation results of an artery consisting of N probability maps. For a given M , the artery is divided into a number $\lceil N/M \rceil$ of sections, where each section is $P = \{P_1 \dots P_M\}$. The TBSS algorithm consecutively takes a voxel probability in P_1 (the first slice in the section), and creates a list of candidate voxel *paths* C , which keep progressing from $m = 1$ until reaching $m = M$. A path $c = \{c_1 \dots c_m\}$ consists of a series of voxel coordinates. Candidate voxels b_m^c for c_m (path c in slice P_m) are chosen from a neighborhood of size B

¹https://www.mit.u-tokyo.ac.jp/projects/tbss/supplementary_material.pdf

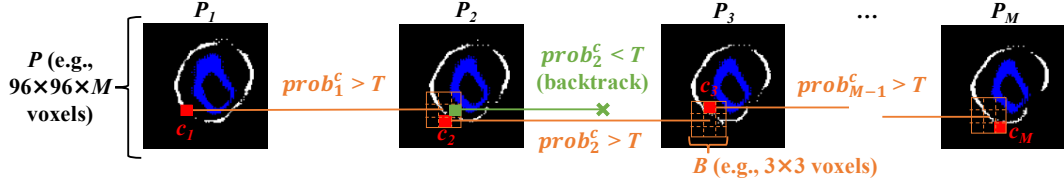


Fig. 2. Construction of a candidate voxel *path* in our TBSS algorithm. For the m^{th} slice of a segmented artery section P , a neighborhood B is set around the most probable voxel coordinates in P_{m-1} , and new paths are searched from there (limited to the S most probable). If the path reaches P_M without exceeding the threshold T , the voxels conforming the path will be included in the reconstructed segmentation.

with center in the coordinates of the previous candidate voxel c_{m-1} . The cumulative probability for the candidate path c is $prob_m^c = \sum_{l=1}^m \log(P_l[c_l])$, for which zero-probabilities are replaced by 10^{-9} to avoid undefined values. Only the voxels whose $prob_m^c > T$ are added to c , and further explored in descending order of probability (to a maximum of S for the given c in P_m). If no $prob_m^c > T$, the algorithm discards the current path and backtracks to the next candidate. When there is no more candidates left, only those who reached the P_M are drawn in the reconstruction R . A schematic of our method can be seen in Fig. 2.

For each section, TBSS is applied to the inner and outer boundaries of P and its reverse P^r , resulting in the reconstructions R^{in} , R^{out} , $R^{r,in}$, $R^{r,out}$. The voxels of these four reconstructions are merged following the aforementioned priority rule to obtain the final reconstruction $R = \{R_1 \dots R_M\}$ of a section. By concatenating all R we obtain the reconstructed artery wall $A = \{A_1 \dots A_N\}$.

Previous coronary wall segmentation methods [5] applied contour finding [13] for each output boundary area. However, TBSS has the effect of thickening uncertain boundaries due to the existence of multiple possible paths through the slice, and thus, simply taking the contour reduces accuracy. To tackle this, we propose using *skeletonization* [14] before finding the contour, which provides the middle “bone” of the reconstructed area. We take the inside contour of the “skeletonized” boundaries, as it empirically tends to be smoother than the outside. This operation is applied to the inner and outer boundaries of every slice in A , and the output of our method is the artery wall contour $O = \{O_1 \dots O_N\}$.

3. EXPERIMENTS

We evaluated our method with a non-public dataset of CCTA scans of 33 patients. From each scan, the CPR volumes for the LAD, LCX and RCA coronary arteries were extracted if available. This sums up to 92 arteries, which comprise 32213 cross-section CPR slices. The separation between voxels in the same CPR slice is $\delta_1 = 0.06mm$ and the separation between slices is $\delta_2 = 0.8mm$. Annotations for the voxels on

each slice were provided by experienced radiologists. The annotation for a voxel v with coordinates ij in the n^{th} slice of an artery is $v_{ij}^n \in \{0, 1, 2\}$, which represent the *background*, *inner boundary* and *outer boundary* classes respectively. Most arteries in the dataset contain anomalies (e.g. stenosis, plaques); slices with an anomaly were annotated as *unhealthy*.

We obtained segmentations for our data via the state-of-the-art method in [5], as older artery segmentation methods do not provide the outer-wall boundary. The resolution of the resulting CPR probability maps is 96×96 voxels. The contours of the segmented boundaries were not perfect, especially in the unhealthy sections. We measured their similarity with the ground-truth annotations via the Hausdorff distance metric, which calculates how close are two curves from each other. Then, we employed our method to reconstruct the segmentations, and remeasured the similarity. The TBSS hyperparameters were chosen empirically using a subset of our dataset; $M = 8$, $T = -0.5$ (inner) and -3 (outer), $S = 9$, and $B = 5 \times 5$. These values serve as a reference for similar unhealthy artery wall datasets.

We compare our TBSS with a baseline and a state-of-the-art work in reconstruction of segmentations, Post-DAE (see Sec. 1). In order to show that modifying the probabilities of single slices is not enough to fix the segmentations, we used Otsu [15] as a baseline, which calculates a global threshold value to classify each pixel in the image. The classification threshold of the original probabilities is 0.5 for both inner and outer boundaries. By applying Otsu, the thresholds for inner and outer boundaries are 0.75 and 0.15, respectively. As for Post-DAE [11], in order to successfully apply it to our boundaries, we replaced their Dice loss with the weighted Hausdorff distance loss as in [5] (refer to the original paper for the remaining parameters). We learned a Post-DAE model and reconstructed separately our inner and outer boundary segmentations through 7-fold cross-validation. The folds were chosen so their number of *unhealthy* slices is similar.

Figure 3 shows the reconstruction results of our experiments for two highly-difficult cases, a bifurcation with plaque (upper half) and a plaque (lower half). In the image, the blue and white areas are the inner and outer boundaries respec-

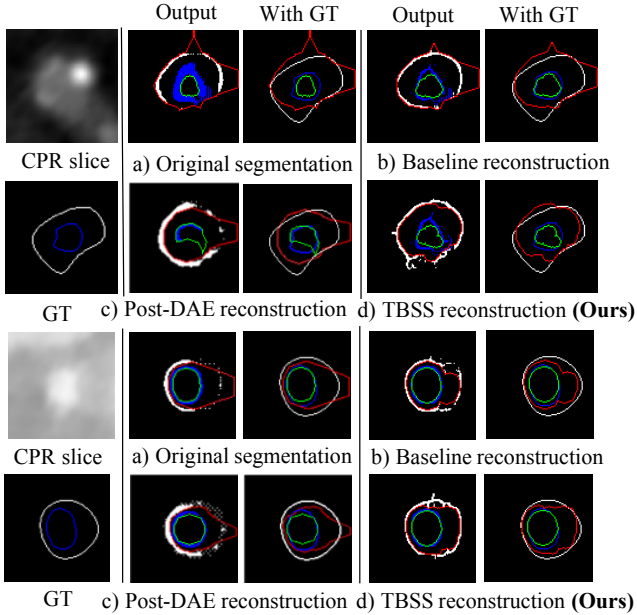


Fig. 3. Comparative results of our evaluation for each method. Inner (blue) and outer (white) boundaries are provided for the method’s output and the ground-truth (GT). The contours extracted for each method’s output (green and red) are overlaid on each image.

tively. For each method, the green and red lines are the contours found for the output inner and outer boundaries respectively. A comparison between the contours and the annotated ground-truth (GT) is provided. In most cases, only the boundaries of the proposed method can provide a closed contour, as they are the most complete (more results on our website²).

We compared these methods via the Hausdorff distance between the boundary contours and the ground-truth annotations, separately for inner and outer boundaries. Table 1 summarizes our results. TBSS not only improved the original segmentation results of [5], but also outperformed the comparison methods. This is more noticeable in *unhealthy* slices, as their boundaries are the most difficult to reconstruct due to the presence of image artifacts. Finally, please note that TBSS is a *reconstruction* method, not a *segmentation* method.

3.1. Discussion

Instead of adding artificial noise to segmentations as in other methods [11], we attempted to reconstruct real defects in segmentations obtained by a state-of-the-art method [5] (Fig. 3 a)). These defects are particularly severe in the outer boundary of slices with bifurcations and/or plaques, in which also the benefits of our method can be better observed. Although the baseline (Fig. 3 b)) improves the original results, it still

²https://www.mi.t.u-tokyo.ac.jp/projects/tbss/supplementary_material.pdf

Table 1. Performance comparison of the proposed reconstruction method with the original segmentation results, a baseline and a state-of-the-art work. The metric used is the averaged Hausdorff distance of all slices (lower is better). An ablation study of the contour-finding (skeletonization) in our method is included.

Method	Inner boundary		Outer boundary	
	Healthy	Unhealthy	Healthy	Unhealthy
Original [5]	5.65	9.1	5.04	10.36
Baseline [15]	4.25	7.85	6.02	9.51
Post-DAE [11]	4.24	6.95	5.23	8.35
TBSS (Ours)	3.6	6.08	3.94	7.1
TBSS w/o skel	5.25	8.82	6	10.29

leaves incomplete areas where voxels have zero or near-to-zero probability of being a boundary. This is because this method relies only on the probabilities of the given slice, and does not leverage the continuity of the artery “tube”. In the case of Post-DAE, since it aims to map the input segmentations to their equivalent anatomically plausible reconstructions, its outputs tend to be round (Fig. 3 c)), like a healthy cross-section. However, this makes this reconstruction method unable to reproduce the large variety of shapes of the segmented arteries. These results confirm that, rather than learning geometry constraints to reconstruct how an artery would look, a better approach is leveraging the probability paths along the artery to produce a reconstruction (Fig. 3 d)).

Due to the small voxel size of the curves, the Hausdorff distance difference among these methods may seem small. However, since a slightly misaligned boundary may lead to a misdiagnosis (e.g., stenosis, positive-remodeling), the improvement achieved by our method is a relevant step towards a real automatic diagnosis of coronary artery diseases. Moreover, these results are an encouraging example of the importance of tackling modern medical image problems by applying ingenuity to algorithms never used before in the field (e.g., beam stack search is normally used in machine translation).

4. CONCLUSIONS

In this paper, we proposed the Tube Beam Stack Search (TBSS) and applied it to the reconstruction of segmentations of coronary artery walls. TBSS leverages the continuity of the artery wall in order to search for high-probability paths. This smooths irregularities and fills “holes” in the artery wall present in segmentation of unhealthy arteries. Compared to a state-of-the-art reconstruction method, TBSS provides the reconstructions that are closest to the ground-truth annotations. To the best of our knowledge, this is the first successful application of the beam-stack search algorithm to medical image. In the future, the applicability of our method will be further explored for reconstructing surfaces in segmentations of different organs.

5. COMPLIANCE WITH ETHICAL STANDARDS

This research study was conducted retrospectively using human subject data collected by Sakurabashi Watanabe Hospital. Approval was granted by the Ethics Committee of RIKEN.

6. ACKNOWLEDGMENTS

No funding was received for conducting this study. The authors have no relevant financial or non-financial interests to disclose.

7. REFERENCES

- [1] Antonio Tejero-de Pablos, Kaikai Huang, Hiroaki Yamane, Yusuke Kurose, Yusuke Mukuta, Junichi Iho, Youji Tokunaga, Makoto Horie, Keisuke Nishizawa, Yusaku Hayashi, et al., “Texture-based classification of significant stenosis in ccta multi-view images of coronary arteries,” in *International Conference on Medical Image Computing and Computer-Assisted Intervention*. Springer, 2019, pp. 732–740.
- [2] Jelmer M Wolterink, Tim Leiner, and Ivana Išgum, “Graph convolutional networks for coronary artery segmentation in cardiac CT angiography,” in *International Workshop on Graph Learning in Medical Imaging*, 2019, pp. 62–69.
- [3] Bin Kong, Xin Wang, Junjie Bai, Yi Lu, Feng Gao, Kunlin Cao, Jun Xia, Qi Song, and Youbing Yin, “Learning tree-structured representation for 3D coronary artery segmentation,” *Computerized Medical Imaging and Graphics*, vol. 80, no. 101688, pp. 1–9, 2020.
- [4] Ahmed M Ghanem, Ahmed H Hamimi, Jatin R Matta, Aaron Carass, Reham M Elgarf, Ahmed M Gharib, and Khaled Z Abd-Elmoniem, “Automatic coronary wall and atherosclerotic plaque segmentation from 3D coronary CT angiography,” *Scientific reports*, vol. 9, no. 1, pp. 1–13, 2019.
- [5] Kaikai Huang, Antonio Tejero-de Pablos, Hiroaki Yamane, Yusuke Kurose, Junichi Iho, Youji Tokunaga, Makoto Horie, Keisuke Nishizawa, Yusaku Hayashi, Yasushi Koyama, and Tatsuya Harada, “Coronary wall segmentation in CCTA scans via hybrid net with contours regularization,” in *Proc. International Symposium on Biomedical Imaging*, 2020, pp. 1743–1747.
- [6] Dong Ping Zhang, *Coronary artery segmentation and motion modelling*, Ph.D. thesis, Imperial College London, 2010.
- [7] Simon Kohl, Bernardino Romera-Paredes, Clemens Meyer, Jeffrey De Fauw, Joseph R Ledsam, Klaus Maier-Hein, SM Ali Eslami, Danilo Jimenez Rezende, and Olaf Ronneberger, “A probabilistic U-Net for segmentation of ambiguous images,” in *Advances in Neural Information Processing Systems*, 2018, pp. 6965–6975.
- [8] Ozan Oktay, Enzo Ferrante, Konstantinos Kamnitsas, Matthias Heinrich, Wenjia Bai, Jose Caballero, Stuart A Cook, Antonio De Marvao, Timothy Dawes, Declan P O’Regan, et al., “Anatomically constrained neural networks (ACNNs): Application to cardiac image enhancement and segmentation,” *IEEE Transactions on Medical Imaging*, vol. 37, no. 2, pp. 384–395, 2017.
- [9] Mahsa Shakeri, Stavros Tsogkas, Enzo Ferrante, Sarah Lippe, Samuel Kadoury, Nikos Paragios, and Iasonas Kokkinos, “Sub-cortical brain structure segmentation using F-CNN’s,” in *Proc. International Symposium on Biomedical Imaging*, 2016, pp. 269–272.
- [10] Konstantinos Kamnitsas, Christian Ledig, Virginia FJ Newcombe, Joanna P Simpson, Andrew D Kane, David K Menon, Daniel Rueckert, and Ben Glocker, “Efficient multi-scale 3D CNN with fully connected CRF for accurate brain lesion segmentation,” *Medical Image Analysis*, vol. 36, pp. 61–78, 2017.
- [11] Agostina J. Larrazabal, Cesar Martinez, and Enzo Ferrante, “Anatomical priors for image segmentation via post-processing with denoising autoencoders,” in *Proc. International Conference on Medical Image Computing and Computer-Assisted Intervention*, 2019, pp. 585–593.
- [12] Rong Zhou and Eric A Hansen, “Beam-Stack Search: Integrating backtracking with Beam Search,” in *International Conference on Automated Planning and Scheduling*, 2005, pp. 90–98.
- [13] Satoshi Suzuki and Keiichi Abe, “Topological structural analysis of digitized binary images by border following,” *Computer Vision, Graphics, and Image Processing*, vol. 30, no. 1, pp. 32–46, 1985.
- [14] D Ballard and C Brown, *Computer Vision*, chapter 8, Prentice-Hall, 1982.
- [15] Nobuyuki Otsu, “A threshold selection method from grey-level histograms,” *IEEE Transactions on Systems, Man, and Cybernetics*, vol. 9, no. 1, pp. 62–66, 1979.